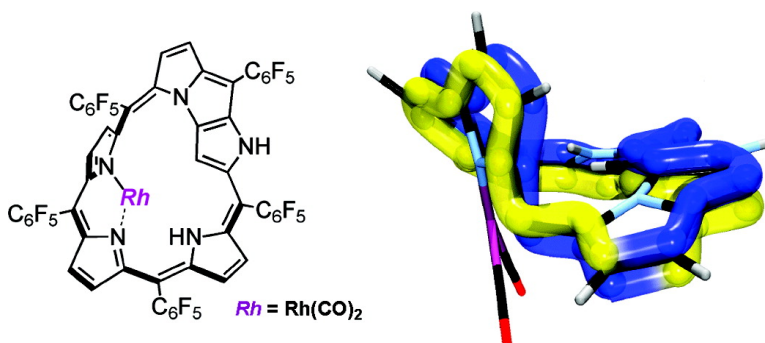


## Möbius Aromaticity in N-Fused [24]Pentaphyrin upon Rh(I) Metalation

Jong Kang Park, Zin Seok Yoon, Min-Chul Yoon, Kil Suk Kim,  
Shigeki Mori, Ji-Young Shin, Atsuhiko Osuka, and Dongho Kim

*J. Am. Chem. Soc.*, **2008**, 130 (6), 1824-1825 • DOI: 10.1021/ja7100483

Downloaded from <http://pubs.acs.org> on December 29, 2008



### More About This Article

Additional resources and features associated with this article are available within the HTML version:

- Supporting Information
- Links to the 9 articles that cite this article, as of the time of this article download
- Access to high resolution figures
- Links to articles and content related to this article
- Copyright permission to reproduce figures and/or text from this article

[View the Full Text HTML](#)



## Möbius Aromaticity in N-Fused [24]Pentaphyrin upon Rh(I) Metalation

Jong Kang Park,<sup>†</sup> Zin Seok Yoon,<sup>†</sup> Min-Chul Yoon,<sup>†</sup> Kil Suk Kim,<sup>†</sup> Shigeki Mori,<sup>‡</sup> Ji-Young Shin,<sup>‡</sup> Atsuhiko Osuka,<sup>\*,‡</sup> and Dongho Kim<sup>\*,†</sup>

Department of Chemistry, Yonsei University, Seoul 120-749, Korea, and Department of Chemistry, Graduate School of Science, Kyoto University, Sakyo-ku, Kyoto, 606-8502, Japan

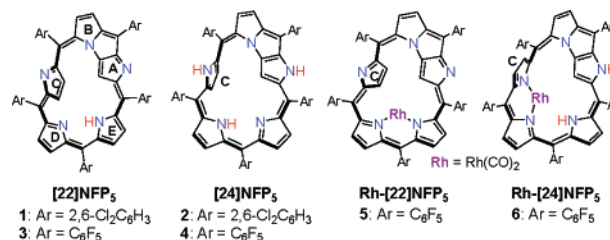
Received November 6, 2007; E-mail: dongho@yonsei.ac.kr; osuka@kuchem.kyoto-u.ac.jp

The concept of Möbius aromaticity that predicts aromatic nature for  $[4n]$ annulenes lying on a twisted Möbius strip is fascinating from both the theoretical and experimental standpoints.<sup>1</sup> Since the first idea on the feasibility of stable Möbius aromatic molecules by Heilbronner early in 1964,<sup>2</sup> there have been speculations on Möbius aromatic molecules as transition states,<sup>3</sup> reactive intermediates,<sup>4</sup> and conformational isomers.<sup>5</sup> Finally we have witnessed the appearance of the first Möbius structure molecule in a seminal work by Herges et al.<sup>6</sup> However, the status of this macrocyclic molecule has encountered disputes over the issue of aromaticity due to its large dihedral angle ( $-107.7^\circ$ ) between the most distorted sites and small NICS value ( $-3.4$  ppm).<sup>7</sup> In annulenic systems, Möbius topology may need a large macrocyclic ring for molecular twisting, where a cis–trans isomerization energy barrier would be very small, thus making “locking in a twisted Möbius structure” very difficult. Very recently, we reported the spontaneous formation of Möbius aromatic molecules upon metalation of expanded porphyrins including [28]hexaphyrin, [32]heptaphyrin, and [36]octaphyrin,<sup>8</sup> whereas [20]porphyrins<sup>9</sup> and [16]porphyrin<sup>10</sup> exhibit severely distorted conformations. The latter results suggest that the tetrapyrrolic porphyrin skeleton is not large enough to implement Möbius twisted topology within a molecule. Now we examine N-fused [22] and [24]pentaphyrins ([22]NFP<sub>5</sub> and [24]NFP<sub>5</sub>) focusing on the possibility of a Möbius aromatic system, since it is important and interesting to characterize the minimum size of pyrrolic macrocycles that can achieve Möbius aromaticity.

N-fused [22] and [24]pentaphyrins **1–4** (Chart 1) that are stable forms of *meso*-aryl pentaphyrins were prepared as reported previously.<sup>11</sup> [22]NFP<sub>5</sub> **1** should exhibit aromatic character according to Hückel rule, when it is planar. This has been supported by its diatropic ring current as seen for the chemical shifts of the inner C–H and N–H protons observed at  $-1.78$  and  $1.27$  ppm, respectively, in the <sup>1</sup>H NMR spectrum. A large negative NICS value of  $-26.7$  ppm calculated at the central position of  $\pi$ -conjugation pathway of **1** also supports its aromatic character. The dihedral angle of the puckered pyrrole ring (ring C) is only  $\sim 30^\circ$  with respect to the entire molecular plane. In contrast, [24]NFP<sub>5</sub> **2** shows the inner NH proton at  $16.98$  ppm and the C2 proton at  $12.01$  ppm and the outer  $\beta$ -protons at  $4\sim 5$  ppm, featuring a distinct paratropic ring current and hence antiaromatic nature for **2**. In accord with this analysis, a positive NICS value ( $+7.71$  ppm) was obtained at the center of **2** (Table 1).

Similar to **1**, the strong diatropic ring current of [22]NFP<sub>5</sub> **3** is evident from its <sup>1</sup>H NMR spectrum that records a large difference of  $11.39$  ppm between the chemical shifts of the inner and outer pyrrolic  $\beta$ -protons ( $\Delta\delta$ ). Thus, **3** can be characterized as a Hückel aromatic molecule with  $22$   $\pi$ -conjugated electrons. In contrast, the <sup>1</sup>H NMR spectrum of [24]NFP<sub>5</sub> **4** exhibits a singlet at  $7.84$  ppm due to the inner C2 pyrrolic  $\beta$ -proton and signals of the outer

**Chart 1.** Molecular Structures of [22] and [24]N-Fused Pentaphyrins<sup>a</sup>



<sup>a</sup> Dicarbonyl group being attached to Rh was omitted for clarity.

**Table 1.** Magnetic, Geometric, and TPA Properties of **1–6**

sample	$\pi$ e <sup>-</sup>	NICS (ppm)	$\Delta R_x$ (Å) <sup>a</sup>	$\Delta R_0$ (Å) <sup>b</sup>	$\Delta\delta$ (ppm) <sup>c</sup>	$\sigma^{(2)}$ (GM) <sup>d</sup>
<b>1</b>	22	$-26.68$	0.095	0.0645	10.62	1430
<b>2</b>	24	$+7.71$	0.167	0.107	$-7.42$	750
<b>3</b>	22	$-28.02$	<i>e</i>	0.0786	11.39	1580
<b>4</b>	24	$-11.75$	0.144	0.0765	$-2.60$	1160
<b>5</b>	22	$-27.11$	0.094 <sup>f</sup>	0.0758	9.17	1720
<b>6</b>	24	$-16.14$	0.100 <sup>f</sup>	0.0803	8.23	1500

<sup>a</sup> Bond length alternation obtained from X-ray crystal structure. <sup>b</sup> Bond length alternation obtained from optimized structure. <sup>c</sup> Difference between the most upfield and the most downfield chemical shifts for  $\beta$ -CH signals ( $\delta_o - \delta_i$ ) for **1**, **3**, **5**, and **6** and vice versa for **2** and **4** in <sup>1</sup>H NMR spectra in CDCl<sub>3</sub> at room temperature. <sup>d</sup> TPA cross-section values were measured at  $1150$  nm for **1** and **3**,  $1600$  nm for **2** and **4**,  $1200$  nm for **5** and **6**, respectively. <sup>e</sup> The analysis of the X-ray data of **3** was not good enough to resolve the structure satisfactorily. <sup>f</sup> The values are the averaged ones of the two independent molecules in the unit cell.

$\beta$ -protons in  $5.58\text{--}6.19$  ppm, which leads to  $\Delta\delta = -2.60$  ppm, hence indicating a weak paratropic ring current. The X-ray crystal structure of **4** shows a significant distortion at the pyrrole C, which is held almost perpendicular to the mean plane of the macrocycle with dihedral angles of  $-122^\circ$  and  $55.7^\circ$  (Figure 1a). It is worthy to note that the large deviation of the pyrrole C is allowed in **4**, presumably due to the less steric interaction of pentafluorophenyl substituents, while larger 2,6-dichlorophenyl substituents in **2** suppress such a ring distortion, hence preserving a relatively planar conformation. This explains the observed antiaromatic character of **2**. It is thus conceivable that the distorted conformation of **4** reduces the strain energy by the fused part of the pyrrole rings. Curiously, the pyrrole C in **4** constitutes the most distorted turning point as it connects the relatively planar N-fused segment consisting of pyrroles A and B and the dipyrromethene segment consisting of pyrroles D and E, where the phase shift in the conjugated  $\pi$ -network might be close to realizing Möbius topology by twisting the conjugated  $p$ -orbitals.

Metalation of **3** with Rh(I) ion in the presence of sodium acetate provided complexes **5** and **6** with  $22$  and  $24$   $\pi$ -electrons, respectively. DDQ oxidation of **6** gave **5** quantitatively via a pivotlike Rh(I)-walk.<sup>11b</sup> In **5**, Rh(I) ion is bound to the nitrogen atoms of

<sup>†</sup> Yonsei University.

<sup>‡</sup> Kyoto University.

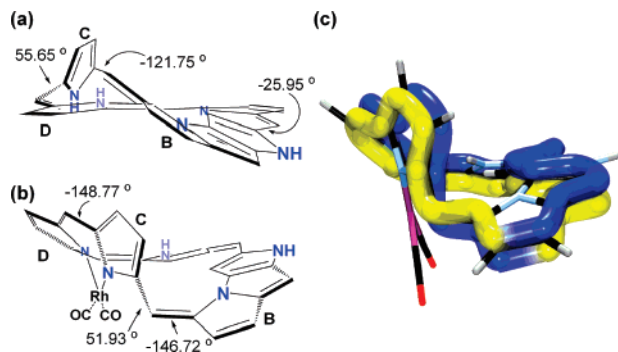


**Figure 1.** (a) Molecular structure of **4** with the three largest dihedral angles obtained from X-ray crystal structure. (b) Molecular structure of **6**, Möbius strip aromatic compound. The values are the average of the two independent molecules in the unit cell. (c) X-ray structure and schematic representation of molecular topology of **6**. The *meso*-pentafluorophenyl groups are omitted for clarity.

pyrroles D and E with an overall planar structure of macrocycle. The aromatic character of **5** has been ascertained from the  $^1\text{H}$  NMR spectrum where the inner  $\beta$ -protons appear at 0.05, 1.16, and 1.62 ppm in the shielded region. Additionally, a small bond-length alternation (BLA) of 0.094 Å from X-ray crystal data and a large negative NICS value of  $-27.11$  ppm at its central position support the Hückel-type aromaticity of **5**.

Remarkably, the structure of Rh(I)-complex **6** has been revealed by single-crystal X-ray diffraction analysis to be a Möbius topology similar to metalated [28]hexaphyrin, [32]heptaphyrin, and [36]octaphyrin.<sup>8</sup> The rigid and planar N-fused tricyclic part (the pyrroles A and B) is nearly planar with the pyrrole E, and the remaining distorted part (the pyrroles C and D) is fixed by Rh(I)-metalation. The pyrrole D constitutes a bent dipyrromethene segment with the pyrrole E, while the pyrrole C is highly distorted. While the pyrrole C in **4** is pointing slightly outward from its  $\pi$ -conjugation pathway, that in **6** is locked inclining inward by Rh(I)-metalation, serving to realize a Möbius topology with reasonable overall conjugation, in which the largest dihedral angles are modest, 51.93° (C10–C11) and  $-146.72^\circ$  (C9–C10). These dihedral angles are considerably smaller than those of **4**, allowing the structure of **6** to satisfy the criteria of Möbius aromaticity asserted by Rzepa.<sup>1a</sup> Importantly, the  $^1\text{H}$  NMR spectrum of **6** reveals a distinct diatropic ring current by displaying the inner  $\beta$ -protons and NH proton at 0.10 and 0.68 ppm in a shielded region, respectively, and the outer  $\beta$ -protons in a slightly deshielded region (7–9 ppm). The large negative NICS value of  $-16.1$  ppm and the BLA value of 0.100 Å also support the aromatic character of this molecule. It should be noted that this BLA value is smaller than 0.157 Å of Möbius structure molecule proposed by Herges et al.<sup>7</sup> and comparable to 0.107, 0.099, and 0.113 Å of Möbius type [28]hexaphyrin, [32]heptaphyrin, and [36]octaphyrin, respectively.<sup>8</sup> Thus, the aromatic character of **6** is apparent from its  $^1\text{H}$  NMR spectrum, a large negative NICS value, and small BLA with Möbius strip topology. Therefore, **6** can be assigned, to the best of our knowledge, as the smallest Möbius aromatic system with a distinct aromatic diatropic ring current characterized so far.

To explore the relationship between two photon absorption (TPA) phenomena and aromaticity demonstrated in our previous work,<sup>12</sup> the TPA cross-section values ( $\sigma^{(2)}$ ) were measured by using the femtosecond Z-scan method.<sup>13</sup> The Hückel aromatic compound **1** shows a TPA value of 1430 GM, almost twice the value for the antiaromatic compound **2** (750 GM). The small  $\sigma^{(2)}$  value of **2** can be ascribed to its antiaromatic character, which is consistent with its almost zero HOMA value (SI). The Hückel aromatic compound

**3** also shows a relatively large TPA cross-section value of 1580 GM, which is similar to that of Hückel aromatic compound **1**. Nonaromatic molecule **4** with a distorted conformation exhibits a larger TPA value of 1160 GM than **2**. Thus, it is conceivable that the larger TPA cross-section value of **4** as compared with that of **2** is arising from its distorted conformation to reduce the strain energy. The Möbius aromatic compound **6** with a distinct diatropic ring current shows the TPA cross-section value of 1500 GM, which is almost comparable to 1720 GM of Hückel aromatic molecule **5**. These results demonstrate that the TPA cross-section values can be used as a quantitative measure of aromaticity in porphyrinoid systems although it still necessitates more theoretical and quantitative analyses.

In summary, NFP<sub>5S</sub> are interesting platforms to realize Hückel aromaticity, Hückel antiaromaticity, and Möbius aromaticity depending on the number of  $\pi$ -electrons, *meso*-substituent, and metalation. Remarkably, the complex **6** has been confirmed as a Möbius aromatic molecule by the crystal structure,  $^1\text{H}$  NMR spectrum, NICS calculation, and TPA cross-section values. This molecule **6** is the smallest Möbius aromatic system with a distinct diatropic ring current. This work demonstrates the potential of our synthetic strategy based on metalation of expanded porphyrins toward Möbius aromatic molecules as well as the possible use of TPA value as a quantitative measure of aromaticity.

**Acknowledgment.** This research was financially supported by the Star Faculty program of the Ministry of Education and Human Resources Development (MEHRD) of Korea (D.K.). The work at Kyoto was supported by a grant-in-aid (A No. 19205006) (A.O.). J.K.P. acknowledges the fellowship of the BK21 program from the MEHRD of Korea.

**Supporting Information Available:** Details of X-ray crystal structure,  $^1\text{H}$  NMR spectrum, X-ray crystal structure, details of synthetic procedure, NICS calculation, HOMA, steady-state absorption, TPA spectra and geometric information. This material is available free of charge via the Internet at <http://pubs.acs.org>.

## References

- (1) (a) Rzepa, H. S. *Chem. Rev.* **2005**, *105*, 3697–3715. (b) Herges, R. *Chem. Rev.* **2006**, *106*, 4820–4842.
- (2) Heilbronner, E. *Tetrahedron Lett.* **1964**, *5*, 1923–1928.
- (3) (a) Zimmerman, H. E. *J. Am. Chem. Soc.* **1966**, *88*, 1564–1565. (b) Moll, J. F.; Pemberton, R. P.; Gutierrez, M. G.; Castro, C.; Karney, W. L. *J. Am. Chem. Soc.* **2007**, *129*, 274–275.
- (4) Mauksch, M.; Gogonea, V.; Jiao, H.; Schleyer, P. v. R. *Angew. Chem., Int. Ed.* **1998**, *37*, 2395–2397.
- (5) Stępień, M.; Latos-Grażyński, L.; Sprutta, N.; Chwalisz, P.; Szterenber, L. *Angew. Chem., Int. Ed.* **2007**, *46*, 7869–7873.
- (6) Ajami, D.; Oeckler, O.; Simon, A.; Herges, R. *Nature* **2003**, *426*, 819–821.
- (7) Castro, C.; Chen, Z.; Wannere, C. S.; Jiao, H.; Karney, W. L.; Mauksch, M.; Puchta, R.; Hommes, N. J. R. v. E.; Schleyer, P. v. R. *J. Am. Chem. Soc.* **2005**, *127*, 2425–2432.
- (8) Tanaka, Y.; Saito, S.; Mori, S.; Aratani, N.; Shinokubo, H.; Shibata, N.; Higuchi, Y.; Yoon, Z. S.; Kim, K. S.; Noh, S. B.; Park, J. K.; Kim, D.; Osuka, A. *Angew. Chem., Int. Ed.* **2008**, *47*, 681–684.
- (9) (a) Pohl, M.; Schmickler, H.; Lex, J.; Vogel, E. *Angew. Chem., Int. Ed. Engl.* **1991**, *30*, 1693–1697. (b) Cissell, J. A.; Vaid, T. P.; Rheingold, A. L. *J. Am. Chem. Soc.* **2005**, *127*, 12212–12213. (c) Cissell, J. A.; Vaid, T. P.; Yap, G. P. A. *J. Am. Chem. Soc.* **2007**, *129*, 7841–7847. (d) Liu, C.; Shen, D.-M.; Chen, Q.-Y. *J. Am. Chem. Soc.* **2007**, *129*, 5814–5815.
- (10) Yamamoto, Y.; Yamamoto, A.; Furuta, S.; Horie, M.; Kodama, M.; Sato, W.; Akiba, K.; Tsuzuki, S.; Uchimaru, T.; Hashizume, D.; Iwasaki, F. *J. Am. Chem. Soc.* **2005**, *127*, 14540–14541.
- (11) (a) Shin, J.-Y.; Furuta, H.; Osuka, A. *Angew. Chem., Int. Ed.* **2001**, *40*, 619–621. (b) Mori, S.; Shin, J.-Y.; Shimizu, S.; Ishikawa, F.; Furuta, H.; Osuka, A. *Chem. Eur. J.* **2005**, *11*, 2417–2425.
- (12) Yoon, Z. S.; Kwon, J. H.; Yoon, M.-C.; Koh, M. K.; Noh, S. B.; Sessler, J. L.; Lee, J. T.; Seidel, D.; Aguilar, A.; Shimizu, S.; Suzuki, M.; Osuka, A.; Kim, D. *J. Am. Chem. Soc.* **2006**, *128*, 14128–14134.
- (13) Sheik-Bahae, M.; Said, A. A.; Wei, T. H.; Hagan, D. J.; Van Stryland, E. W. *IEEE J. Quantum Electron.* **1990**, *26*, 760–769.

JA7100483